Mining Science, vol. 31, 2024, 61–79

www.miningscience.pwr.edu.pl

Mining Science

(Previously Prace Naukowe Instytutu Gornictwa Politechniki Wroclawskiej, ISSN 0370-0798)

ISSN 2300-9586 (print)
ISSN 2353-5423 (online)

Received January 7, 2024; Reviewed; Accepted August 25, 2024

STUDY ON ROCK-BREAKING CHARACTERISTICS OF CONSTANT SECTION AND SPHERICAL TOOTH HOB WITH THE AID OF SLOT PRODUCED BY WATER JET

Xuhui ZHANG[1]*, Kang LONG[1], Tao TAN[1],
Sijia LI[2], Lian Lian TAN[3]

[1] College of Engineering and Design, Hunan Normal University, Changsha, 410081, China
[2] Shuda College, Hunan Normal University, Changsha 410017, China
[3] Hunan Lianzhi Technology Co., Ltd. Changsha Hunan 410219, China

Abstract: In order to analyze and compare the rock-breaking characteristics of constant section hob (CS hob) and spherical tooth hob (ST hob) with the aid of slot produced by water jet, a linear cutting models of granite using two types of hobs under the slot conditions were established using the finite element method. The cutting forces, rock-breaking states, and specific energy consumption of hobs were calculated. The research results revealed that during the cutting process, both types of hobs can induce surface and internal tensile cracks in the rock. There exists a critical cutting width for each type of hob, within which the tensile cracks can extend to the slot, promoting rock fragmentation and generating large rock chips. Under the slot conditions, the vertical and rolling forces on ST hob were found to be smaller than those on CS hob. Moreover, the cutting force of the hob can be greatly decreased by using the proper cutting width. When the hob can effectively utilize the slot for breaking rock, their specific energy consumption is significantly lower than it would be without the slot, which greatly improves the effectiveness of cracking rocks. Additionally, it was discovered that the specific energy consumption of the ST hob was lower than the CS hob's, indicating that with the aid of slot produced by water jet, the rock-breaking efficiency of ST hob is higher than that of CS hob.

Keywords*: *spherical tooth hob, constant section hob, TBM, slot, water jet

* Corresponding author: xuhui@hunnu.edu.cn (X. Zhang)

doi: 10.37190/msc243104

1. INTRODUCTION

With the progress and development of society, the development of underground spaces and resources has received increasing attention. Tunnel Boring Machine (TBM) are the main equipment used for underground space development, relying primarily on disc-shaped hob for breaking rock(Farrokh et al. 2024). However, hard rock conditions can lead to issues like limited rock-breaking effectiveness, quick hob wear, and tool axis detachment(Zhang et al. 2024a), leading to frequent tool replacements, increased construction costs, and extended construction periods (Lin et al. 2024).

To improve rock-breaking efficiency of TBM hob, scholars have explored the influence of various parameters on rock-breaking effects. Cho et al. (2013) carried out experiments to study the rock breaking characteristics of hob cutting granite. Abu Bakar et al. (2014) carried out rock-breaking experiments to study the particle size of rock debris and rock-breaking characteristics of hob. Labra et al. (2017) proposed a discrete/finite element method for cutting rock with a TBM hob. Entacher and Schuller (2018) investigated the influence of foliation angle on rock breaking characteristic. Thyagarajan and Rostami (2024) studied the influence of variable penetration on rock breaking load of hob. Zhang et al. (2022a) used the Discrete Element Method to investigate the effects of confining pressure and cutter spacing on rock-breaking performance of TBM hob. Ning et al. (2020)studied the influence of different blade widths on rock-breaking force and specific energy consumption of TBM. Li et al. (2022) examined the effects of rotation speed and penetration depth on the effectiveness of the TBM hob in breaking rocks using the Finite Element Method. Zhang et al. (2022b) studied the rock cutting characteristics of spherical-tooth hob under different penetration. Hu et al. (2022) investigated the effects of hob spacing and hob height difference on specific energy consumption and crack propagation.

To further advance the rock-breaking performance of the TBM hob, some assisted rock-breaking methods have emerged, such as microwave assisted rock-breaking method (Hassani et al. 2016), laser assisted rock-breaking method (Zhang et al. 2022c), and water jet assisted rock-breaking method (Zhang et al. 2024b). Water jet assisted rock-breaking involves cutting rocks through water jets to create slots, and hob roll and break rocks with the aid of these slots. High rock-breaking efficiency is one of the benefits of using water jet assisted rock-breaking over other assisted rock-breaking methods. In addition, it also has advantages such as small vibration and impact, and sustainable environmental protection, so it has been widely studied and discussed in recent years. Ciccu and Grosso (2014) conducted study on the use of water jets to assist in breaking rocks, and came to the conclusion that water jets can enhance the effectiveness of hobs. Han et al. (2023) designed a new experimental machine combining water jet assisted rock-breaking method and investigated the effects of changing water jet spray position, height, and pressure on rock-breaking efficiency. Cheng et al. (2021; 2022) examined the TBM hob's penetrating behavior in the slot condi-

tion caused by the high-pressure water jet. Luo et al. (2023) conducted experimental research on the rock-breaking mechanism of hob with the assistance of water jet.

Constant section hob (CS hob) and spherical tooth hob (ST hob) are the two primary types of hobs used in the TBM field, as depicted in Fig. 1. The ST hob has a row of sphere-shaped teeth arrayed on its blade, in contrast to the CS hob. It may be seen from the analysis above those current studies mostly concentrate on the rock-breaking properties of the CS hob assisted with water jet, with few studies comparing the rock-breaking characteristics of the ST hob assisted with water jet. In other words, the difference of rock-breaking mechanism between CS hob and ST hob assisted with water jet is unclear. therefore, the rock-breaking characteristics of two hobs assisted with water jet are compared on the basis of finite element simulations in this study, which can provide insights for parameter optimization and tool design in water jet assisted rock-breaking in TBM field.

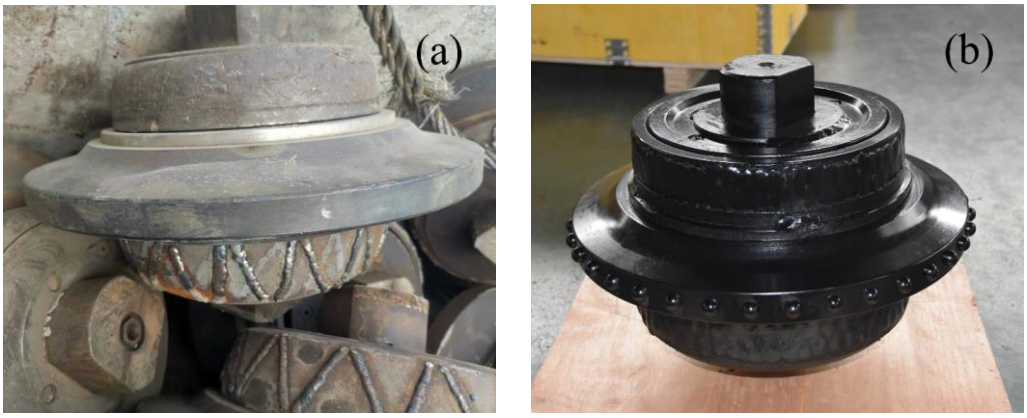

Fig. 1. The disc hob: (a) CS hob, (b) ST hob

2 DESIGN OF SIMULATION

2.1. BASIC PARAMETERS OF ROCK SAMPLE AND THE TWO TYPES OF HOBS

For the rock-breaking of hob assisted with water jet, it is to first use the water jet to cut a slot on the rock to generate a free surface in advance, then, based on the prefabricated free surface, the rock is cut with hob. In the simulations, the slot and the free surface has been prefabricated, as shown by the pre-cut slot in Fig. 2. With the aid of water jet, a slot with a depth of 35 mm and a width of 5 mm is created on the rock surface firstly in the cutting model. The distance from the left boundary of the rock to the slot is 50 mm, as shown in Fig. 2a. the hob is located to the right of the slot. The distance between the center of the hob and the slot is defined as the cutting width, de-

noted as S. Because the rock-breaking ability of the two hobs is different, the rock-breaking characteristics of the two hobs cannot be well reflected under the same range of cutting width, so we selected different change range for two types of hobs. Specifically, the ST hob has cutting width options of 10, 20, 30, 40, 50, and 60 mm, while the CS hob has cutting width options of 50, 60, 70, 80, 90, and 100 mm. The hob cut along a direction of 400 mm in length. Considering the common values of hob penetration depth in TBM engineering, a penetration depth of 6 mm is set for both types of hobs in the simulation. The hob size selected is a common 17-inch hob with a diameter of 432 mm. The blade width of two hobs is 12 mm. The radius, height, and spacing of the spherical teeth on ST hob is 6 mm, 6 mm, and 22.6 mm, respectively. During the simulation, the hob is treated as rigid bodies, therefore they do not undergo deformation during the cutting process. Contact force acting on hob is shown in Fig. 2b, And name it vertical force (FV), rolling force (FR), and lateral force (FS).

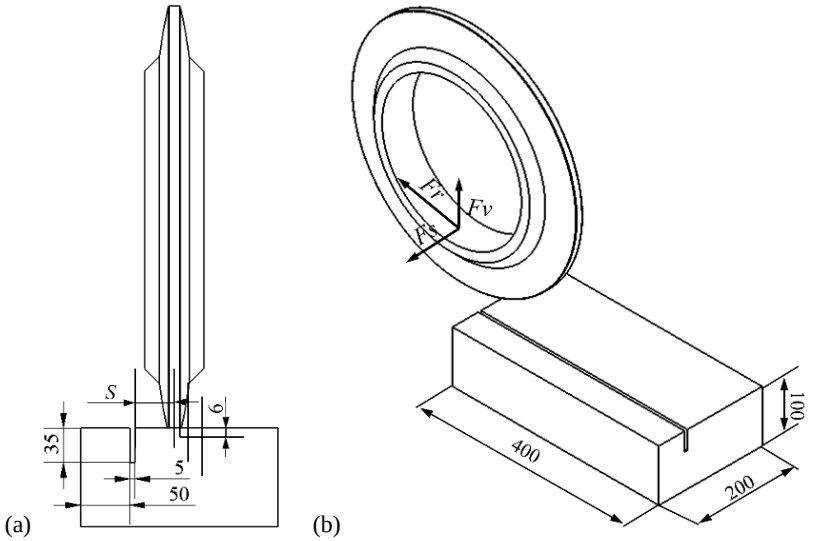

Fig. 2. Hob linear cutting rock model: (a) front view; (b) three-dimensional view

2.2. CONSTITUTIVE PROPERTY OF ROCK SAMPLE

The rock selected in this study is a common granite encountered in TBM excavation. Uniaxial compressive tests and Brazilian splitting tests were conducted on granite specimens, as shown in Fig. 3. The experimental equipment used was a microcomputer servo-controlled pressure testing machine, which is primarily used for testing the mechanical properties of high-strength solid materials and can perform tests such as rock tensile tests, uniaxial compression tests, and indentation tests. Figure 4 shows a fractured granite specimen obtained from the experiment. The compressive strength of gran-

ite determined from the laboratory test is around 141 MPa, the tensile strength is around 11.8 MPa, and the elastic modulus is around 13.2 GPa.

Fig. 3. Microcomputer-controlled servo hydraulic pressure testing machine

Fig. 4. Fractured granite specimen

To simulate the behavior of granite material in this work, the RHT constitutive model was used. The RHT model (Wang et al. 2021), which can simulate the internal crack propagation and damage process of rock materials under impact loading. To match the mechanical properties of the rock material, a uniaxial compression model for the rock was established, as shown in Fig. 5. The mesh size of the model was set to 4 mm. By adjusting the relevant parameters of the RHT model, the simulated mechanical characteristics of the model were made close to the actual experimental results. Results from the experiment and those from simulation are contrasted in Fig. 6, indicating that the calibrated parameters of the RHT model are reliable. The key parameters of the calibrated granite RHT model are listed in Table 1.

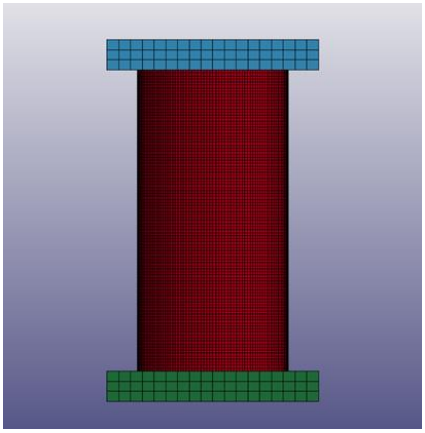

Fig. 5. Finite element mesh model of granite under uniaxial compression

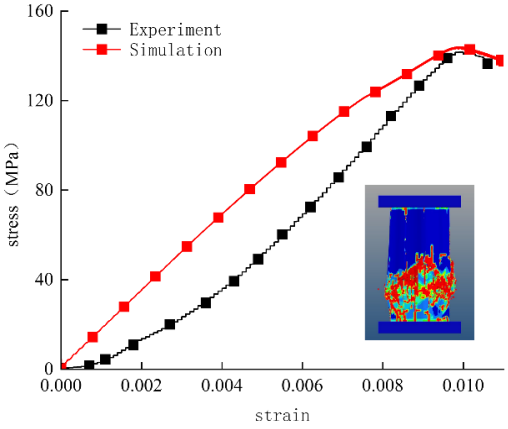

Fig. 6. Comparison between simulation and experimental results

Table 1. Partial model parameters of granite RHT

Parameters and units	Value	Parameters and units	Value
f_c [MPa]	141	α_0	1.1
ρ_0 [kg/m^3]	24200	A_1 [GPa]	86.71
A_2 [GPa]	145.67	A_3 [GPa]	89.03
β_c	0.0106	β_t	0.0144
B_0	1.68	B_1	1.68
T_1 [GPa]	86.71	T_2 [GPa]	0
G [GPa]	11.8	$\varepsilon_0^c / 10^{-8}$ ms^{-1}	3.0
$\varepsilon_0^t / 10^{-9}$ ms^{-1}	3.0	$\varepsilon_0^c / 10^{22}$ ms^{-1}	3.0
$\varepsilon^t / 10^{22}$ ms^{-1}	3.0	N	0.56

2.3. MESH DIVISION AND BOUNDARY CONDITIONS

The established model was imported into the simulation program for meshing and boundary condition settings, as shown in Fig. 7. The use of a finer mesh in the simulation usually leads to more accurate simulation results, so a portion of the rock that touches the hob is given a finer mesh with a size of 2 mm. while the regions further away from the hob were meshed with a size of 4 mm. The simulation was performed based on the SPG algorithm. Smooth particle Galerkin (SPG) algorithm is an efficient and accurate algorithm, which is suitable for failure and damage analysis of elastomer and semi-brittle materials. It can deal with problems from low speed to high speed, with the advantages of high accuracy. Non-reflective boundary constraints were ap-

plied to all surfaces of the rock model except for the upper surface and the pre-cut slot. The non-reflective boundary conditions can eliminate the influence of rock size and boundary effects on the hob-rock cutting process. In the simulation, a translational velocity with a value of 20 m/s was applied to the hob to simulate its cutting action on the rock.

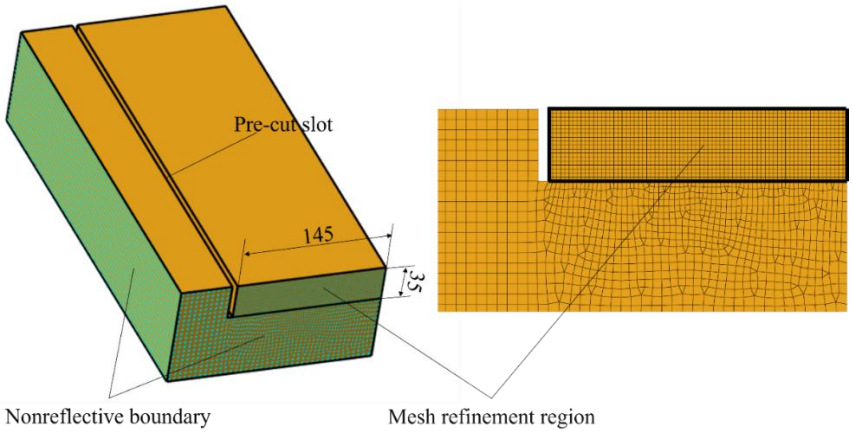

Fig. 7. Setting of rock boundary conditions and mesh division

3. RESULTS AND ANALYSIS

3.1. ANALYSIS OF TWO TYPES OF HOBS' ROCK-BREAKING PROCESS

CS hob and ST hob dynamic rock-cutting processes with the aid of slot are analyzed and contrasted in this section. Figure 8 shows the dynamic cutting processes of the CS hob with cutting widths of 70 mm and 100 mm.

Based on the crack propagation states shown in the surface Fig. 8a1 and the cross-section Fig. 8a4, it can be observed that there are significant differences in the crack distribution between the slot side and the non-slot side during the rock-breaking process. As shown in Fig. 8a2, When the hob is cutting, it contacts the rock and then penetrates it, resulting in obvious tensile cracks on the rock surface. From Figure 8a5, it can be observed that severe damage occurs to the rock below the hob as it penetrates the rock, leading to the formation of a crushing zone. In the crushing zone, tensile fractures form and spread toward the slot. As shown in Fig. 8a3, as the hob moves, obvious groove below the hob appears on the rock surface, and more tensile cracks occur on the side of the rock surface close to the slot. These surface tensile cracks extend to the slot, which can promote the surface fragmentation of the rock. Based on cross-section Fig. 8a6, it can be observed that internal cracks generated by the hob in

the crushing zone extend to the rock slot, causing big rock fragments to spall between the hob and the slot.

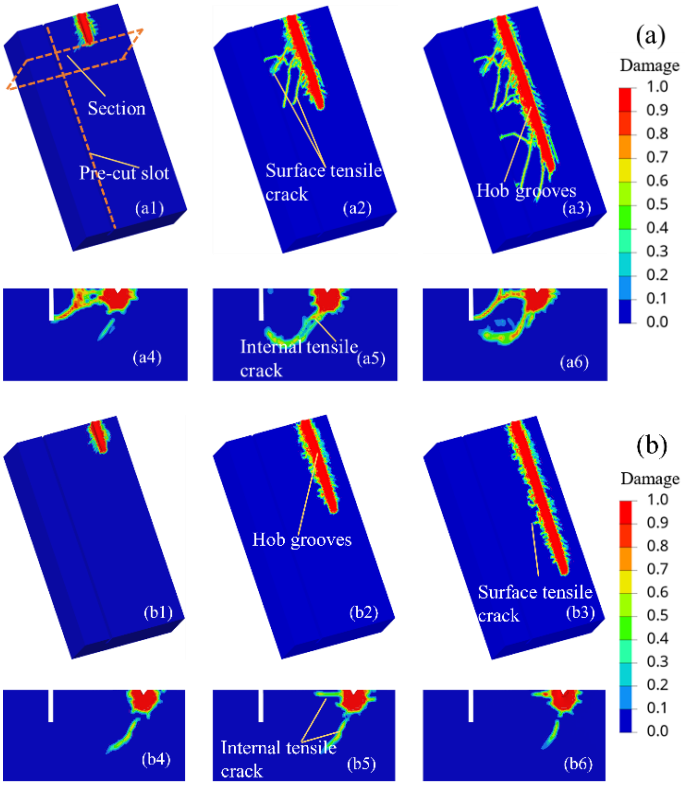

Fig. 8. Dynamic process of rock-breaking by CS hob:
(a) cutting width 70 mm, (b) cutting width 100 mm

Figure 8b shows the rock-breaking process using a CS hob with a cutting width of 100 mm. Based on the crack propagation states shown in Fig. 8b1 and the cross--section Fig. 7b4, when the cutting width increases to 100 mm, the promoting effect of the slot produced by the water jet on rock-breaking almost disappears. The crack patterns on the slot side and the non-slot side become similar, and the direction of internal tensile crack propagation in the rock still tends towards the slot, but the trend is not as pronounced as that observed at a cutting width of 70 mm. As shown in Fig. 8b2, surface cracks can also occur on both sides of the groove, but there are fewer and shorter surface cracks, leading to a less effective surface fragmentation. From the cross-section Fig. 8b5, it can be observed that fewer tensile cracks are generated inside the rock. From Figure 8b3, compared to a cutting width of 70 mm, a significant groove is still formed on the rock surface after cutting by the hob at a cutting

width of 100 mm, as shown in Fig. 8b6. Due to the increased cutting width, internal tensile cracks cannot extend to the slot, resulting in the inability to produce large rock fragments. This indicates that the influence of the slot on rock-breaking is minimal under this condition.

Based on the analysis above, for the CS hob, choosing an appropriate cutting width, such as 70 mm, has a positive promoting effect on rock-breaking. At this cutting width, the rock surface and the inside appear obvious tensile cracks between the hob and the slot. When a large number of cracks can extend to the slot, large rock fragments can be produced. However, when the cutting width is too large, the cracks generated by the hob during cutting are not able to extend to the slot, and the slot produced by the water jet cannot effectively promote rock-breaking.

Based on the crack propagation states shown in the Fig. 9a1 and the cross-section Fig. 9a4, it can be observed that under a cutting width of 30 mm, the length of the tensile cracks on the side close to the slot is greater than that on the non-slot side when using a ST hob. As shown in Fig. 9a2, under the combined action of the ST hob and the slot, surface tensile cracks extending from the damaged area to the slot are generated, promoting surface fragmentation of the rock. Additionally, the length of the tensile cracks on the side close to the slot is greater than that on the non-slot side. From Fig. 9a5, when the hob penetrates the rock, internal tensile cracks propagate from the crushing zone towards the slot. When utilizing the ST hob to cut rock, as seen in Fig. 9a3, The rock surface cut by the hob produces discontinuous broken areas. With the intrusion of the hob, approximately spherical crushing zones are generated in the rock with the center directly below the tooth. Based on Fig. 9a6, it can be concluded that the rock-breaking process is influenced by the slot. Internal cracks produced by the hob in the crushing zone propagate to the slot, causing rock to spall and resulting in massive rock fragments.

Figure 9b shows the rock-breaking process using a ST hob with a cutting width of 60 mm. Based on the crack propagation states shown in Fig. 9b1 and the cross-section Fig. 9b4, when the cutting width increases to 60 mm, the promoting effect of the slot produced by the water jet on the rock-breaking process using the ST hob almost disappears. The surface crack patterns on the slot side and the non-slot side become similar, and internal tensile cracks in the rock almost disappear. As shown in Fig. 9b2, under this cutting width, the surface cracks are not obvious and the surface rock-breaking effect is poor. From the cross-section Fig. 9b5, it can be observed that only a small number of tensile cracks are generated inside the rock, and there is no obvious trend in crack propagation direction. Fig. 9b3 reveals that when the cutting width is 60 mm, a broken region still formed on the rock after hob cutting. As shown in Fig. 9b6, due to the increased cutting width, it becomes difficult for internal tensile cracks to initiate, resulting in the inability to produce large rock fragments. This indicates that the promoting effect of the slot on rock-breaking disappears under this cutting width for the ST hob.

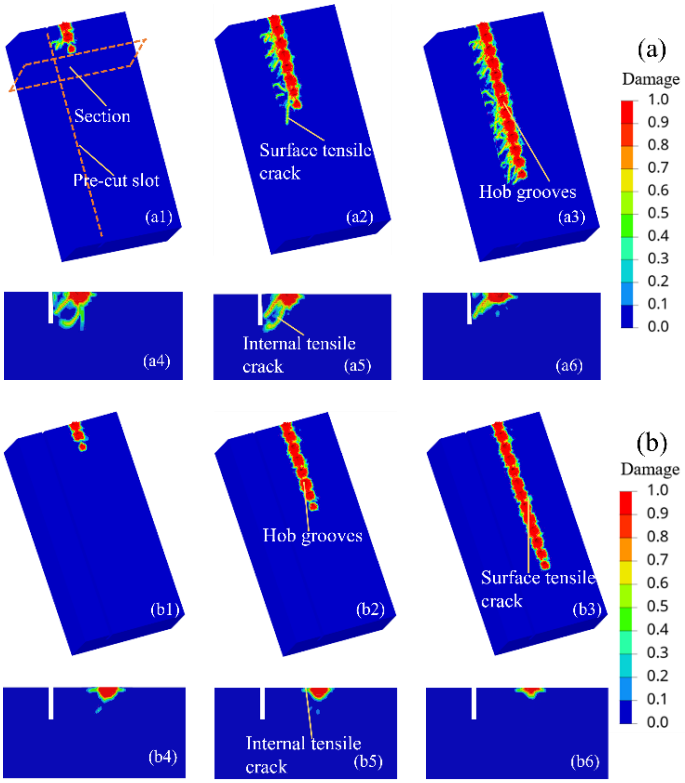

Fig. 9. Dynamic process of rock-breaking by ST hob:
(a) cutting width 30 mm, (b) cutting width 60 mm

In summary, comparing the rock-breaking processes using the two types of hobs, it is found that the cracks generated by the CS hob through rolling cutting are generally longer than those generated by the ST hob, indicating that the crack propagation capability of the CS hob is stronger. Under the appropriate cutting width, the slot produced by the water jet can promote the generation of tensile cracks on the surface and inside the rock between the hob and the slot, resulting in production of large rock fragments. However, when the cutting width is too large, the slot cannot promote crack generation effectively, thus unable to effectively promote rock-breaking with the hob.

The variations of the vertical force exerted by the two hobs under different cutting widths, are depicted in Figs. 10a and 10b. It can be shown that, no matter the type of hob, the vertical force during breaking process caused by the hob exhibits certain fluctuations at different cutting widths, it fits the hob's intermittent pattern of rock-breaking. Furthermore, it shows that the vertical force exerted by both the CS hob and the ST hob does not drop to zero during the cutting process. This shows

that during the cutting process, the hob is constantly in touch with the rock, and there is still reaction force even if the rock is broken below the hob. For the CS hob at different cutting widths, it can be seen in Fig. 10a, it is evident that the vertical force at a cutting width of 100 mm is generally greater than that at a cutting width of 70 mm. Based on the analysis of the rock-breaking process shown in Fig. 8a, it can be inferred that the slot at a cutting width of 70 mm can promotes crack propagation. Under such promoting conditions, the hob influenced by the slot requires less force to achieve better rock-breaking results.

According to Fig. 10b, similar to the CS hob, the vertical force of the ST hob when the cutting width is 30 mm is generally less than the vertical force when the cutting width is 60 mm. Similarly, this is because the crack can expand to the slot when the cutting width is 30 mm, so the force of the hob can be reduced. In addition, compared with the CS hob, as shown in the Fig. 10a, the vertical force of the ST hob fluctuates more intensively with the displacement of the hob. This is because the spherical teeth on the ST hob ring are arranged according to a certain distance, when the ST hob cuts the rock, the spherical teeth invade the rock in turn, and separate from the rock in turn, so the vertical force of the spherical teeth fluctuates significantly with the change of displacement.

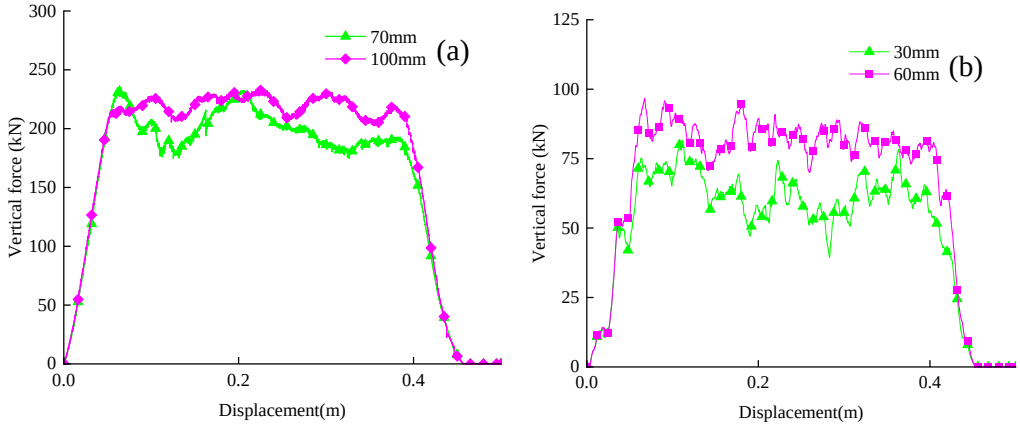

Fig. 10. Variation of vertical force on hob with displacement: (a) CS hob; (b) ST hob

In addition, according to Figs. 10a, and 10b, it can be inferred that the vertical force of CS hob is significantly higher than that of the ST hob. This is since the rock-breaking process with the ST hob is a discontinuous process. When the spherical teeth of the hob penetrate the rock, the stress rapidly increases until it reaches its peak, and then the rock fractures, causing the stress to be released. Therefore, the peak force of the ST hob cannot continue to increase. It may be deduced from the study in this section that under specific cutting widths, the slot can promote rock-breaking induced by two

hobs. However, the analysis does not provide the critical cutting widths corresponding to the two types of hobs. It will be discussed in next sections.

3.2. COMPARISON OF ROCK-BREAKING STATE

To contrast the impacts of CS hob and ST hob on rock-breaking at different cutting widths, the surface and internal rock-breaking states at various cutting widths are summarized in Figs. 11 and 12.

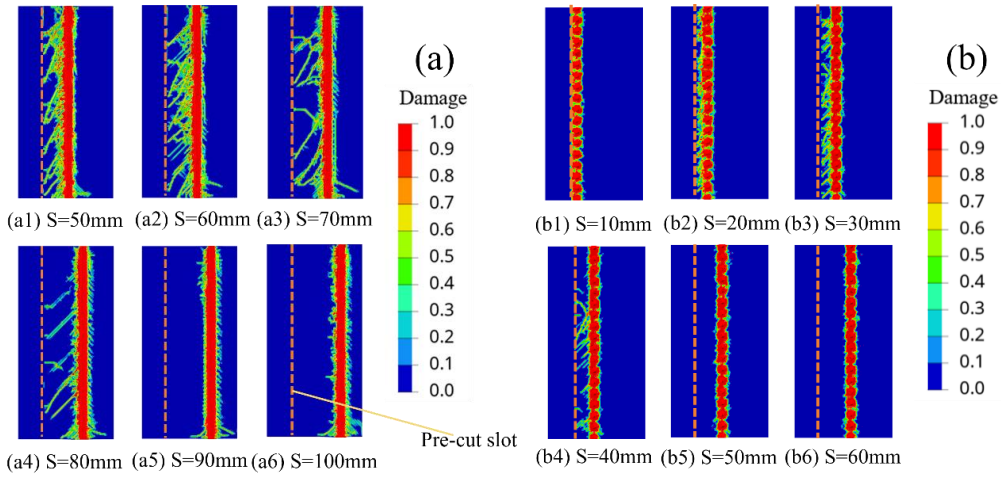

Fig. 11. Surface rock-breaking state under different cutting widths:
(a) CS hob, (b) ST hob

As shown in Figs. 11a1–11a4, significant tensile cracks appear on the surface between the CS hob and the slot when the cutting widths are 50 mm, 60 mm, 70 mm, and 80 mm, while fewer significant surface tensile cracks can be seen on the hob's non-slot side. The internal cross-sections of the rock after cutting with the CS hob at different cutting widths are shown in Fig. 12a. Tensile cracks originating from the crushed zone extend towards the slot for cutting widths ranging from 50 mm to 80 mm, as shown in Figs. 12a1–12a4. However, when the cutting width reaches 90 mm, as shown in Fig. 12a5 the propagation trend of internal tensile crack caused by CS hob cutting gradually disappeared, indicating that the slot produced by water jet has little influence on the rock-breaking process using the ST hob in this cutting width. From Figure 12a, it can be inferred that with increasing cutting width until it reaches 70 mm, the tensile cracks extending from the crushed zone can reach the slot. However, as the cutting width continues to increase, the internal cracks cannot extend to the slot, as shown in Fig. 12a4. To make use of the assisted rock-breaking effect of the slot, a reasonable cutting

width should be set. In this study, the appropriate cutting width for cutting granite using the CS hob is determined to be about 70 mm.

From Figures 11b1–11b4, it can be concluded that the ST hob produces significant surface tensile cracks between the slot and the hob at cutting widths of 10 mm, 20 mm, 30 mm, and 40 mm, respectively, while fewer tensile cracks are observed on the non-slot side of the surface. The internal cross-sections of the rock after cutting with the ST hob at different cutting widths are shown in Fig. 12b. Figures 12b1–12b3 show that when the cutting width is 10, 20, 30 mm, there are internal tensile cracks in the rock that can expand to the slot. When the cutting width increases to 40 mm, as shown in Fig. 12b4, the ST hob still produces significant tensile cracks, but the cracks cannot extend to the slot. This indicates that the slot produced by water jet has little influence on the rock-cutting process using the ST hob in this cutting width, and it is difficult to promote rock tensile fracturing and the generation of large rock fragments. Therefore, the reasonable cutting width for cutting granite using the ST hob in this study is determined to be 30 mm.

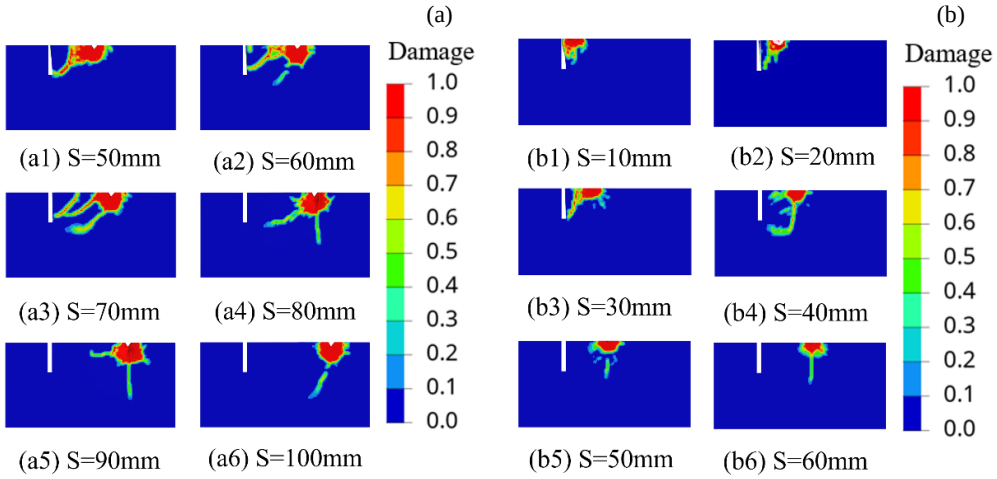

Fig. 12. Rock-breaking state sectional view under different cutting widths:
(a) CS hob, (b) ST hob

Based on Figures 11 and 12, it can be observed that the CS hob and the ST hob exhibit similar characteristics in terms of the influence of cutting width on the formation of tensile cracks and large rock fragments. As cutting width is increased, the number of surface tensile fractures steadily decreases, and when the cutting width of both types of hobs reaches a certain limit, the rock fragmentation state on both sides of the hob is almost the same. In other words, only a small number of tensile cracks are generated on the rock surface and in the internal structure, and the tensile cracks on the side of the slot cannot extend to the slot, indicating that the slot cannot promote

the generation of tensile cracks. Compared with the CS hob as shown in Fig. 11, the critical cutting width of the ST hob is smaller, and the tensile crack generated by the CS hob in the rock-breaking process is longer than that of the ST hob.

3.3. COMPARISON OF ROCK-BREAKING FORCE

The CS hob and ST hob's average rock-breaking forces at various cutting widths are shown in Fig. 13. From Fig. 13a, it can be observed that the vertical force of the CS hob is much greater than the other two forces. The change trend of average forces with respect to cutting width is as follows: The CS hob's rolling force and vertical force steadily increase. and then stabilize with the increase of the cutting width, while the lateral force initially decreases and then stabilizes. As analyzed in Section 3.2, as shown in Figs. 11a and 12a, the number of tensile cracks generated on the rock surface and internal sections by the hob gradually decreases with the increase of cutting width. When the cutting width reaches a certain point, the internal tensile cracks cannot extend to the slot, resulting in a reduced volume of rock fragment and difficulty in stress release. Therefore, the rolling force and vertical force steadily increase. When the cutting width between the CS hob and the slot exceeds 70 mm, the promoting effect of the slot on surface and internal tensile cracks diminishes. In other words, the rock fragmentation process under such large cutting width (more than 70 mm) using the CS hob approaches that without the assistance of the slot. Thus, the average vertical force of the CS hob becomes stable at these cutting widths. Analyzing the variation of lateral force with cutting width for the CS hob, as shown in Fig. 13a, it can be observed that the lateral force decreases with the increase of cutting width and then stabilizes. The lateral force decreases from 6.17 kN at a cutting width of 50 mm to 1.95 kN at a cutting width of 80 mm. When the cutting width is above 80 mm, the lateral force stabilizes. This is because, when the cutting width is less than 80 mm, a large number of tensile cracks are generated on the rock surface and internal sections between the hob and the slot, as shown in Figs. 11a1–11a3, and in Figs. 12a1–12a3. The other side of the hob is unaffected by the slot, resulting in an unbalanced load on the hob and
a significant lateral force. With the increase in cutting width, the promoting effect of the slot on the generation of tensile cracks gradually weakens, and the rock-breaking difference on both sides of the CS hob decreases, leading to a decrease in lateral force. When the cutting width exceeds 80 mm, there is no obvious difference in the rock fragmentation state on both sides of the CS hob, on both sides of the CS hob, and the reaction force becomes balanced on both sides of the hob, resulting in a small lateral force.

As shown in Fig. 13b, it can be found that the average forces of the ST hob during rock-breaking process exhibit a similar trend to that of the CS hob. When comparing the vertical force, rolling force, and lateral force for the same cutting width, the verti-

cal force is much greater than the other two forces. The change trend of the average forces with respect to cutting width for the ST hob is as follows: the vertical force and rolling force increase with the increase of the cutting width, and after reaching a certain value, they gradually stabilize. Referring to the analysis in Section 3.2 and Fig. 11b, with the increase in cutting width, the promoting effect of the slot on rock fragmentation weakens, resulting in the internal tensile cracks cannot extend to the slot, a reduced volume of rock fragment and difficulty in stress release. Therefore, the rolling force and vertical force steadily increase. As shown in Fig. 13b, as cutting width increases, the ST hob's lateral force shows a tendency of decreasing, and when the cutting width exceeds 40 mm, the lateral force stabilizes. Similar to the CS hob, when the cutting width is less than 40 mm, a large number of tensile cracks are generated on the rock surface and internal sections on one side of the hob close to the slot, as shown in Figs. 11b1–11b3, and in Figs. 12b1–12b3. The other side of the hob is not affected by the slot, resulting in an unbalanced force on the hob and a significant lateral force. With the increase in cutting width, the promoting effect of the slot on the generation of tensile cracks gradually weakens, and the rock-breaking difference on both sides of the hob decreases, leading to a decrease in lateral force. When the cutting width exceeds 40 mm, there is no obvious distinction in the rock fragmentation condition on either side of the hob, and the reaction force balances out on both sides, causing the lateral force to decrease.

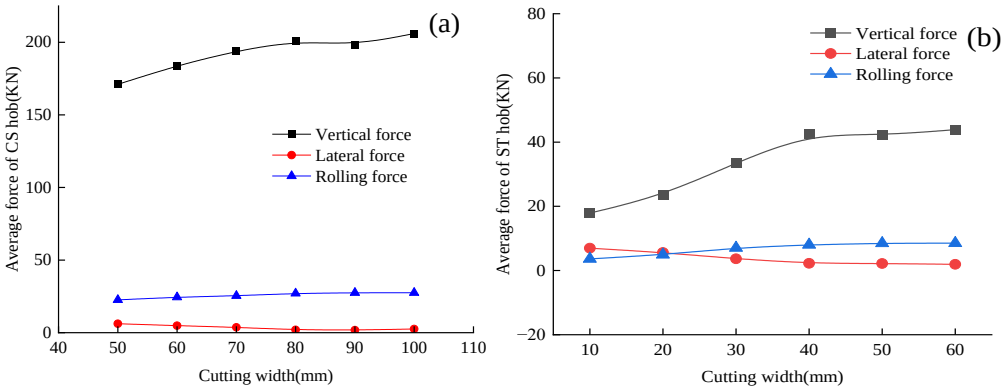

Fig. 13. Three-direction average force of two hobs under different cutting widths: (a) CS hob, (b) ST hob

In summary, comparing the average forces of the CS hob and ST hob as shown in Fig. 13, it can be concluded that although the cutting widths are different, the CS hob's vertical force and rolling force are both much higher than the ST hob's, the average

lateral forces of the two types of hobs are relatively close during the rock cutting process.

3.4. COMPARISON OF SPECIFIC ENERGY CONSUMPTION

The phrase "specific energy consumption" relates to how much energy a hob uses to break up unit volume of rocks (Qiao 2018). Higher rock-breaking efficiency is indicated by a lower value of specific energy consumption. Figure 14 illustrates the variation of specific energy consumption with cutting width for the CS hob and the ST hob.

The CS hob exhibits a trend of initially decreasing, then increasing, and eventually stabilizing specific energy consumption with the increase of cutting width. As analyzed in Subection 3.2 and shown in Fig. 12a, when the cutting width is within 70 mm, the tensile cracks generated by the CS hob can extend to the slot. The size of the rock fragments also rises with cutting breadth, which results in a reduction in specific energy consumption and an increase in the CS hob's rock-breaking effectiveness. The slot's promoting impact on rock-breaking, however, nearly completely vanishes when the cutting width approaches 70 mm. The tensile cracks on the surface and inside the rock near the slot side fail to extend to the slot, preventing the formation of large rock fragments, resulting an increase in specific energy consumption. The CS hob's minimal specific energy consumption is about 9.82. MJ/m^3 at a cutting width of 70 mm. while the specific energy consumption increases to 21.2 MJ/m^3 when the cutting width reaches 80 mm. The former is approximately 46% of the latter. In short, when the CS hob can use the slot effectively to break rock, its rock-breaking efficiency will be greatly improved.

Similarly, for the ST hob, when the cutting width is less than 30 mm, with increasing cutting width, the specific energy consumption steadily drops until it reaches its lowest point at a cutting width of 30 mm. This is because the tensile cracks can extend to the slot, and as the cutting width increases, the rock fragment size increases, thereby reducing specific energy consumption and improving rock-breaking efficiency. However, combined with Fig. 12b, when the cutting width exceeds 30 mm, the tensile cracks fail to extend to the slot, and the promoting effect of the slot almost disappears. This prevents the formation of large rock fragments, resulting in an increase in specific energy consumption. The ST hob's minimal specific energy consumption is about 6.97 MJ/m^3 at a cutting width of 30 mm, but it increases to 12 MJ/m^3 when the cutting width increases to 40 mm. The former is approximately 58% of the latter. Since then, due to the disappearance of assisted rock-breaking effect for slot, the continuous increase of cutting width can not affect the specific energy consumption of ST hob. By comparing the variations of specific energy consumption for the CS hob and the ST hob, it can be concluded that the ST hob has a lower specific energy consumption than the CS hob. The average specific energy consumption for the CS hob is 16.73 MJ/m^3, while the average specific energy consumption for the ST hob

is approximately 10.36 MJ/m^3. In this sense, the ST hob can not only has a smaller cutting force but also has a higher rock-breaking efficiency compared with the CS hob.

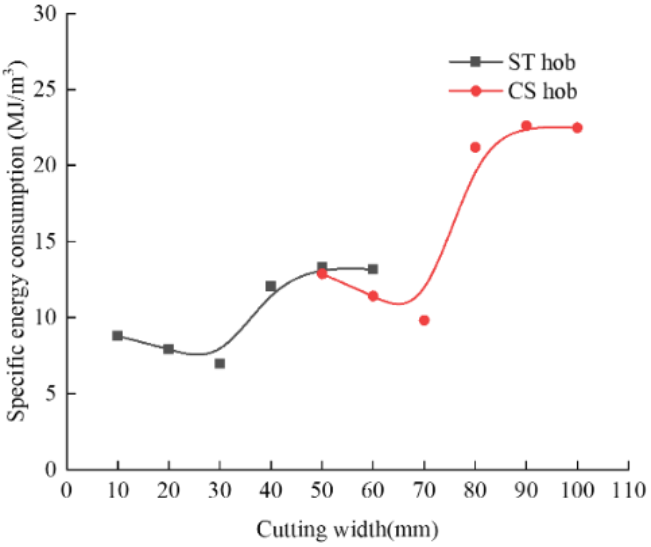

Fig. 14. Variation of specific energy consumption at different cutting width

4. CONCLUSION

This study investigated the rock-breaking characteristics of ST hob and CS hob with the aid of slot produced by water jet. The following conclusions were drawn regarding the variations of cutting width on the rock-breaking process, rock-breaking force, rock-breaking states, and rock-breaking efficiency:

1. When the cutting width does not exceed 70 mm for CS hob and 30 mm for ST hob, both hobs produce surface and internal tensile cracks that propagate to the slot, causing the formation of large rock fragments. However, when the cutting width exceeds these thresholds, the internal tensile cracks fail to reach the slot, and the slot produced by water jet exhibits insignificant promoting effects on rock-breaking.
2. With the increase of cutting width, the vertical force and rolling force of the CS hob and ST hob show an initial increase, followed by stabilization, while the lateral force exhibits a decreasing trend. When the cutting width is within 70 mm for CS hob and 30 mm for ST hob, significant reduction in cutting force of hob can be achieved with the aid of slot.
3. The vertical force and rolling force of ST hob are smaller than those of CS hob, the lateral force of two types of hobs is similar. In addition, the crack propaga-

tion ability of CS hob is stronger than that of ST hob.

4. With the aid of slot produced by water jet, the specific energy consumption for both CS hob and ST hob initially decreases, then increases, and eventually stabilizes as the cutting width increases. The specific energy consumption is lower for ST hob compared to CS hob. The results suggest that the optimal cutting widths for achieving the highest rock-breaking efficiency are 70 mm for CS hob and 30 mm for ST hob.

ACKNOWLEDGEMENTS

The research was supported by the National Natural Science Foundation of China (Grant No. 52005179), the Scientific Research Project of Hunan Education Department (Grant No. 20C1153), and the Natural Science Foundation of Hunan Province (Grant No. 2020JJ5365), and the Innovation and Entrepreneurship Training Plan Program for College students in Hunan Province (No. S202312652008).

DECLARATION OF INTERESTS

The authors declare that they have no known competing financial interests or personal relationships that could have appeared to influence the work reported in this paper.

REFERENCES

ABU BAKAR M.Z., GERTSCH L.S., ROSTAMI J., 2014, *Evaluation of Fragments from Disc Cutting of Dry and Saturated Sandstone*, Rock Mechanics and Rock Engineering, 47, 1891–1903.

CHENG J., WANG Y., WANG L., LI Y., HU B., JIANG Z., 2021, *Penetration behaviour of TBM disc cutter assisted by vertical precutting free surfaces at various depths and confining pressures*, Archives of Civil and Mechanical Engineering, 21.

CHENG J., YANG S., HAN W., ZHANG Z., JIANG Z., LU J., 2022, *Experimental and numerical study on the indentation behavior of TBM disc cutter on hard-rock precutting kerfs by high-pressure abrasive water jet*, Archives of Civil and Mechanical Engineering, 22, 1–23.

CHO J., JEON S., JEONG H., CHANG S., 2013, *Evaluation of cutting efficiency during TBM disc cutter excavation within a Korean granitic rock using linear-cutting-machine testing and photogrammetric measurement*, Tunnelling and Underground Space Technology, 35, 37–54.

CICCU R., GROSSO B., 2014, *Improvement of Disc Cutter Performance by Water Jet Assistance*, Rock Mechanics and Rock Engineering, 47, 733–744.

ENTACHER M., SCHULLER E., 2018, *Angular dependence of rock cutting forces due to foliation*, Tunnelling and Underground Space Technology, 71, 215–222.

FARROKH E., ROKHY H., LOTFI D., 2024, *Evaluation of side forces for gauge cutters through LS-DYNA 3D numerical simulations*, Arabian Journal of Geosciences, 17.

HAN W., FU J., LUO X., GUO L., XIA Y., HE S., 2023, *A New Linear Cutting Experimental Machine for Disc-Cutter Rock Breaking with High-Pressure Water Jets Assisted*. KSCE Journal of Civil Engineering, 27, 2666–2675.

HASSANI F., NEKOOVAGHT P.M., GHARIB N., 2016, *The influence of microwave irradiation on rocks for microwave-assisted underground excavation*, Journal of Rock Mechanics and Geotechnical Engineering, 8, 1–15.

HU M., ZHANG B., LI B., CAO W., 2022, *Using Discrete Element Method to Study the Rock Breaking Effect of Worn TBM Cutters*, Geotechnical and Geological Engineering, 40, 2843–2856.

LABRA C., ROJEK J., OÑATE E., 2017, *Discrete/Finite Element Modelling of Rock Cutting with a TBM Disc Cutter*, Rock Mechanics and Rock Engineering, 50, 621–638.

LI X., ZHANG H., BAI Y., ZHANG X., 2022, *Factor analysis and numerical simulation of rock breaking efficiency of TBM deep rock mass based on orthogonal design*, Journal of Central South University, 29, 1345–1362.

LIN L., LI R., LUO X., XIA Y., 2024, *Comparative study on the rock breaking performance of constant cross section disc cutter and inserted tooth disc cutter for cutting granite*, Tunnelling and Underground Space Technology, 150, 105840.

LUO X., ZHANG J., YANG F., HE F., XIA Y., 2023, *Research on the hard rock cutting characteristics of disc cutter under front-mounted water jet precutting kerf conditions*, Engineering Fracture Mechanics, 287, 109330.

NING B., XIA Y., LIN L., ZHANG X., HE Y., LIU Y., 2020, *Experimental study on the adaptability of cutters with different blade widths under hard rock and extremely hard rock conditions*, Acta Geotechnica, 15, 3283–3294.

QIAO S, 2018, *Performance Evaluation of Different Pick Layouts on Bolter Miner Cutting Head*, Journal of Mining Science, 54, 969–978.

THYAGARAJAN M.V., ROSTAMI J., 2024, *Study of cutting forces acting on a disc cutter and impact of variable penetration measured by full scale linear cutting tests*, International Journal of Rock Mechanics and Mining Sciences, 175, 105675.

WANG H., WANG Z., WANG J., WANG S, WANG H., YIN Y. et al., 2021, *Effect of confining pressure on damage accumulation of rock under repeated blast loading*, International Journal of Impact Engineering, 156, 103961.

ZHANG K., LIU W., YAO X., PENG C., LIU J., ZHENG X., 2022c, *Investigation on Two-Step Simulation Modeling Method for Rock Breaking by TBM Disc Cutters Assisted with Laser*, KSCE Journal of Civil Engineering, 26, 2966–2978.

ZHANG Q., ZHU Y., DU C., DU S., SHAO K., JIN Z. et al., 2022a, *Dynamic Rock-Breaking Process of TBM Disc Cutters and Response Mechanism of Rock Mass Based on Discrete Element*, Advances in Civil Engineering, 2022.

ZHANG X., LONG K., TAO T., LIAO Y., LI J., LIAO J., 2024a, *Research on Adaptability of CS and BT Hobs to Break Soft and Hard Rock*, KSCE Journal of Civil Engineering.

ZHANG X., LONG Z., LIAO Y., LONG J., LIU J., 2022b, *Investigation on rock cutting characteristics of spherical-tooth hob*, Mining Science, 29, 121–144.

ZHANG X., TAN T., LI M., LIAO Y., TIAN Y., LIAO J., 2024b, *Research on rock breaking behaviors of different TBM hobs under grooving condition produced by water jet*, Engineering Failure Analysis, 162, 108373.